**Table 1.** Equilibria of transfer from vapor to cyclohexane at 25°C. The values are from the solubilities collected by Wilhelm and Battino (*20*), except that for water, which is from the present experiments, and that for cyclohexane, which is calculated from the vapor pressure of cyclohexane at 25°C.

| Solute | $\Delta G_{vap \rightarrow chx}$ (kcal/mol) |
|---|---|
| Helium | 2.17 |
| Neon | 1.94 |
| Argon | 0.69 |
| Methane | 0.23 |
| Krypton | 0.02 |
| Water | −0.04 |
| Xenon | −0.82 |
| Ethane | −0.94 |
| Propane | −2.05 |
| Butane | −2.77 |
| Cyclohexane | −4.35 |

(Table 1). Molecules smaller than water, such as helium and hydrogen, strongly prefer the vapor phase. Larger molecules, such as xenon or propane, much prefer the hydrocarbon phase. Krypton, with a molecular surface area similar to that of water (*15*), also shows a distribution coefficient of approximately unity for transfer from the vapor phase to cyclohexane (*16*).

Is water, in equilibrium with liquid water, expected to occupy a nonpolar cavity created in the interior of a protein by mutation? An approximate, but decisive, answer to this question can be obtained for any nonpolar region in the interior of a protein molecule whose properties are assumed to resemble those of a liquid hydrocarbon (*17*). In equilibrium with liquid water, cyclohexane contains $1.5 \times 10^{-3}$ M water. At that concentration, one water molecule is present in a volume of about $1.1 \times 10^{6}$ Å$^3$ of solvent. Accordingly, the probability of finding a water molecule in any particular volume of solvent just large enough to accommodate a water molecule would be 1 in 60,000 (*18*). If a cavity had been created in the solvent before water entered (in an operation comparable with the creation of a cavity in a protein by mutation), then that chance would increase. The cost in free energy of opening a cavity of this size in a protein molecule is roughly 0.7 kcal (*19*). After correction for this effect, the chance of finding a water molecule that is in equilibrium with liquid water, in a preformed nonpolar protein cavity just large enough to accommodate water, is of the order of 1 in 20,000. That probability would increase markedly, of course, if the water molecule were able to make contact with a polar group or with another water molecule.

These results lead to the inference that a single water molecule is highly unlikely to be found in a small nonpolar cavity in a protein. Individual water molecules pass between the vapor phase and a nonpolar condensed phase, however, with remarkable equanimity.

## REFERENCES AND NOTES


1. R. Wolfenden, *Science* **222**, 1087 (1983).
2. A. Finkelstein, *Water Transport Through Lipid Bilayers, Pores, and Plasma Membranes* (Wiley-Interscience, New York, 1987), pp. 94–106.
3. A. Fersht, *Biochemistry* **27**, 1577 (1988).
4. R. Wolfenden and W. M. Kati, *Acc. Chem. Res.* **23**, 209 (1991).
5. A. E. Eriksson *et al.*, *Science* **255**, 178 (1992).
6. R. C. Wade, M. H. Mazo, J. A. McCammon, F. A. Quiocho, *Biopolymers* **31**, 919 (1991).
7. R. Varadarajan and F. M. Richards, *Biochemistry* **31**, 12315 (1992).
8. A. M. Buckley, K. Henrick, A. R. Fersht, *J. Mol. Biol.* **234**, 847 (1993).
9. W. D. Harkins and Y. C. Cheng, *J. Am. Chem. Soc.* **43**, 35 (1921).
10. S. R. Ungemach and H. F. Schaefer III, *ibid.* **96**, 7898 (1974).
11. S. D. Christian, A. A. Taha, B. W. Gash, *Q. Rev. Chem. Soc.* **24**, 20 (1970).
12. E. N. Dorsey, *Properties of Ordinary Water-Substance* (Reinhold, New York, 1950).
13. W. W. Washburn in *International Critical Tables* (McGraw-Hill, New York, 1928), vol. 3, p. 210.
14. Other experiments show that single water molecules behave similarly toward aliphatic hydrocarbon solvents ranging from $C_5$ to $C_{17}$ and toward perfluorocarbon solvents ranging from $C_6$ to $C_{10}$, with equilibrium constants ranging from 0.7 to 1.6 for transfer from the dilute vapor phase to the organic solvent (R. Wolfenden and A. Radzicka, unpublished results).
15. The molecular surface area of both molecules, as estimated by the method of J. L. Pascual-Ahuir and E. Silla [*J. Comput. Chem.* **6**, 1047 (1990)] is about 35 Å$^2$ (D. Doyle, unpublished results).
16. The comparable behavior of water and krypton may appear surprising. However, earlier work has shown that vapor-to-cyclohexane distribution coefficients of other molecules are remarkably insensitive to differences in solute polarity [A. Radzicka and R. Wolfenden, *Biochemistry* **27**, 1664 (1988)].
17. The possibility that such a resemblance exists, at least to a limited extent, is supported by the observation that differences in side-chain free energies of transfer from cyclohexane to water are numerically similar to changes in free energy of denaturation that result from mutating nonpolar side chains in protein interiors [G. D. Rose and R. Wolfenden, *Annu. Rev. Biophys. Biomol. Struct.* **22**, 381 (1993)].
18. This probability was estimated by dividing the approximate volume of a water molecule, 20 Å$^3$ [taken as the volume of a sphere with a surface area of 35 Å$^2$ (*15*)], into $1.1 \times 10^6$ Å$^3$, the volume of distribution of each water molecule in water-saturated cyclohexane.
19. The cost in free energy of opening a nonpolar cavity in the interior of a protein molecule is probably in the neighborhood of 20 cal/Å$^2$ (*5*), equivalent to an equilibrium constant of 0.3 for opening a cavity with an area of 35 Å$^2$ (*15*). If the cost in free energy of opening such a cavity had been paid in advance, then water's tendency to enter the cavity would be enhanced by a factor of about 3.
20. E. Wilhelm and R. Battino, *Chem. Rev.* **73**, 1 (1973).
21. This work was supported by grant GM-18325 from the National Institutes of Health. We are grateful to D. Doyle for calculating the molecular surface area of water.


11 March 1994; accepted 16 June 1994

# Surface Dating of Dynamic Landforms: Young Boulders on Aging Moraines

Bernard Hallet and Jaakko Putkonen

**The dating of landforms is crucial to understanding the evolution, history, and stability of landscapes. Cosmogenic isotope analysis has recently been used to determine quantitative exposure ages for previously undatable landform surfaces. A pioneering application of this technique to date moraines illustrated its considerable potential but suggested a chronology partially inconsistent with existing geological data. Consideration of the dynamic nature of landforms and of the ever-present processes of erosion, deposition, and weathering leads to a resolution of this inconsistency and, more generally, offers guidance for realistic interpretation of exposure ages.**

The surface of the globe is continually changing because of the interplay between degradational processes that tend to lower the landscape and constructional processes that tend to elevate it. Understanding these processes and the rates at which they operate is of value to both the scientific community and society, because the form and stability of land surfaces impact and are impacted by many human activities. Considerable information about rates of surficial processes can be extracted from ages of landform surfaces. Until recently, these ages have been approximated by dating material above or beneath the surface or by estimating the time required to account for the observed degree of weathering and erosional modification of the surface. In general, it has not been possible to date landform surfaces directly and quantitatively. In this context, the development of exposure-age dating of rock surfaces based on the progressive accumulation of diverse isotopes produced by collisions with cosmic rays (*1*, *2*) has been welcomed by geomorphologists. In this report, we focus attention on dating moraines because they have been the subject of several cosmo-

Quaternary Research Center and Department of Geological Sciences, University of Washington, Seattle, WA 98195, USA.

genic isotope studies and because they constitute the most prominent terrestrial records of glacial history. Accurate dating of these landforms is critical to the reconstruction of the temporal and spatial variability of past climates on land.

Realistic interpretation of exposure ages requires an understanding of two sets of processes. First are processes that alter cosmogenic isotope concentrations in rocks that have been exposed to the elements and to cosmic rays for a given duration. These include boulder erosion, which tends to proceed inward from the surface, thereby removing material most enriched in cosmogenic isotopes (*2–4*), and prior exposure of boulders before incorporation into the landform, which yields an excess of cosmogenic isotopes (*5*). Second are those processes that alter the duration of exposure and render it different from the landform formation age; heretofore they have received little consideration and are examined in this report.

In dating moraines by exposure ages, the duration of subaerial exposure of boulders on moraine crests is implicitly equated with the age of the moraine itself. However, in general there is no simple relation between moraine age and either the exposure age of boulders or their degree of weathering. Boulders initially situated on the moraine surface as ice retreats tend to remain there, but fine-grained sediment removal by wind, water, and slow downslope movement causes additional boulders to emerge at the moraine surface as this surface is lowered. These newly exposed boulders were previously sheltered from cosmic rays and will thus attain exposure ages that are younger than the moraine formation age. Boulders at or near the ground surface break down and eventually disappear because of weathering. Thus, the age distribution of surface boulders is a function not only of moraine age but also of the competing effects of moraine erosion and boulder weathering, which respectively add and subtract surface boulders.

Well-developed moraines on the east side of the Sierra Nevada, California, consisting largely of granitic till have received considerable attention (*6–11*). Their relative ages have been determined from diverse moraine properties, including the degree of soil development; the abundance and weathering characteristics of boulders on moraine surfaces; moraine shape that tends to smooth out with time because of erosion; and, in places, the superposition of moraines that reveals their ordering in time.

The glacial chronology of the Bloody Canyon–Walker Creek area is controversial because a study by Phillips and colleagues (*5*) who used cosmogenic chlorine-36 yielded dates that disagreed with prior accepted estimates. At this site during the most recent glaciations, ice flowed along a different path than it did previously, providing a rare record of older moraine crests that otherwise would have been overridden. Moreover, the crosscutting relations and superposition provide direct indications of relative ages among five distinct lateral moraine sets (*10*). Bloody Canyon and Walker Creek are at a mean elevation of 2350 m in the semiarid Great Basin physiographic province (*12*).

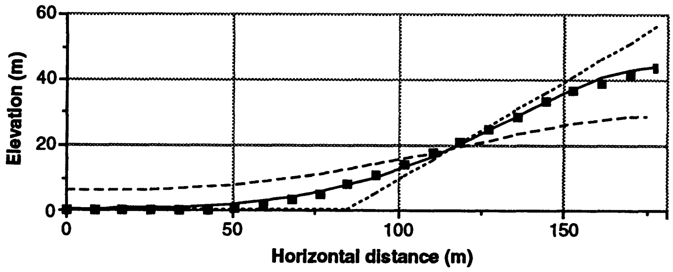


**Fig. 1.** Data points are measurements (*22*) along half of the transverse topographic profile of a Tioga lateral moraine estimated to be 22,000 years old (no vertical exaggeration). Starting with a 31° slope (dotted), the model yields the profile of the Tioga moraine (solid) and, for comparison, the profile of a hypothetical 100,000-year-old moraine (dashed). Although the moraine crest is often selected for dating purposes because the low slopes suggest geomorphic stability, the crest is where the greatest ground-lowering occurs; it is calculated to be 16 m and 28 m for the 22,000- and 100,000-year-old moraines, respectively. These lowering rates are broadly consistent with sparse field data (*16*). Rate constants for topographic diffusivity are given in the text.

The weathering of boulders has been studied in the Bloody Canyon–Walker Creek area and elsewhere on the east side of the Sierra Nevada (*8, 13*). The influence of local erosion exposing subsurface boulders on exposure-age distributions has recently been explored (*14*) without consideration of weathering. In addition, the progressive topographic degradation of moraines has been well documented in the field (*15, 16*) and has been the subject of theoretical analysis (*17*). These studies provide the foundation for our modeling.

In our model, a moraine flattens and widens with time as fine-grained sediment is transferred downslope from the moraine crest, exposing previously buried boulders there. Topographic evolution is dictated by the spatially nonuniform downslope motion of soil, defined here as including the loose, glacially derived rock debris that makes up the bulk of moraines (*18*). For example, if more soil exits from one particular domain than enters, the average elevation of that domain must decrease. Thus, the conservation of soil leads to an expression relating the rate of change of the local surface elevation, $dz/dt$, to the divergence of soil flux, $q$

$$\partial z/\partial t = -\partial q/\partial x \qquad (1)$$

where $x$ is the horizontal distance in a plane perpendicular to the moraine axis (*19*).

No studies of slope processes have been conducted on the Bloody Canyon–Walker Creek moraines, but modeling can be guided by studies of slope evolution in areas with similar climate and substrate composition: erosional scarps on alluvial fans in Idaho (*20*) and fault and erosional scarps on alluvial fans in the Great Basin (*21*). In both studies, the degradation of small escarpments up to about 10 m in height was viewed as resulting dominantly from progressive and intermittent downslope soil motion. This movement is known as soil creep and arises from a diversity of processes that recurrently move soil particles including wind, rain splash, freeze and thaw cycles, and plant and animal activity. Moreover, these studies show that the topographic evolution of scarps can be modeled quantitatively as a simple diffusional process much like heat conduction. The analog of thermal diffusivity is the topographic diffusivity, $\kappa$, which is the volume of soil moving downslope per unit time and per unit length transverse to the slope divided by the slope inclination, $\partial z/\partial x$. The simplest relation expressing the general increase in soil flux with slope steepness is

$$q = -\kappa \partial z/\partial x \qquad (2)$$

For slopes a few meters long, $\kappa$ typically ranges between $10^{-2}$ to $10^{-4}$ m$^2$/year over a wide spectrum of areas, climates, and alluvial substrates (*21*). For longer slopes, as high as 20 m on erosional scarps in alluvium, the value for $\kappa$ increases linearly with distance downslope (*20*). To treat the evolution of lateral moraines, which in Bloody Canyon range in heights from about 50 to 200 m, we assume that topographic diffusivity takes the form

$$\kappa = \alpha + \beta x \qquad (3)$$

where $\alpha$ and $\beta$ are site-specific constants. The transport equation relating soil flux to slope, together with the expressions for the

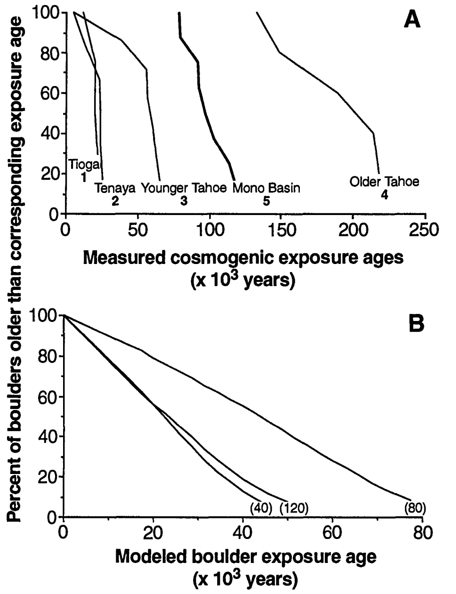


**Fig. 2.** Age distribution of boulders on a moraine crest. (**A**) Measured cosmogenic $^{36}$Cl ages (5) and stratigraphic order shown with numerals from youngest (1) to oldest (5) (*10*). The Mono Basin moraine is oldest stratigraphically but has intermediate exposure ages. This inconsistency may be apparent only; as shown in (**B**), modeled mean exposure ages do not increase monotonically with moraine age. The assigned moraine age, in thousands of years, is given in parentheses at the bottom of each trace. The form evolution model was applied to a Mono Basin moraine with 0.5-m-diameter boulders; the use of larger boulders would result in older surface exposure ages, in closer accord with the results shown in (B). Boulder attrition rates are poorly known; representative values were taken to be $1.6 \times 10^{-5}$ m/year below the ground surface and $2.3 \times 10^{-6}$ m/year above it.

conservation of material and for κ, leads to a generalized diffusion equation for topographic evolution

$$\frac{\partial z}{\partial t} = \frac{\partial}{\partial x}\left(\kappa \frac{\partial z}{\partial x}\right) = \kappa \frac{\partial^2 z}{\partial x^2} + \beta \frac{\partial z}{\partial x} \qquad (4)$$

This equation can readily be solved numerically with a finite-difference approximation. For simplicity, the moraine is assumed to have an initial triangular cross section with both sides slightly gentler than the angle of repose. This initial condition seems reasonable in view of the sharp-crested form typical of lateral moraines recently exposed by glacier retreat. However, moraines quickly relax from their sharp-crested form, and hence this assumption has little influence on long-term topographic evolution. We complete the problem formulation by introducing a boundary condition specifying that material transferred from the upper portion of the moraine reaches its final destination directly downslope. This condition applies to much of the moraine, except locally where streams have incised and evacuated sediments from the foot slope.

This diffusion model produces moraine transverse topographic profiles in excellent agreement with observed forms (Fig. 1), which supports the notion (*16*) that lateral moraine profiles can be useful indicators of moraine age. The present form of a moraine of known age and initial shape can be used to evaluate the time-averaged transport parameters for this site. We assume that the age of the youngest Tioga moraine is 22,000 years (*10*) and that it had symmetrical slopes initially inclined at 31°. A close match between computed and observed (*22*) profiles requires the rate constants of the spatially varying topographic diffusivity to be $\alpha = 1.2 \times 10^{-2}$ m$^2$/year and $\beta = 1.6 \times 10^{-4}$ m/year (Fig. 1). Sums of least-square differences were used to determine these best values of α and β with a resolution of approximately 20%. Near the crest, κ approaches α and is comparable with the larger values obtained for ~10-m fault scarps in the Great Basin (*21*). The part of the model presented above yields the surface-lowering rate at a moraine crest, which permits determination of the rate at which new boulders emerge at the surface of the moraine crest as they are unearthed, and the length of time any particular boulder is subjected to subsurface and subaerial weathering.

The weathering rate of most medium-grained granitic boulders on the surface of alluvial fans and moraines on the east side of the Sierra Nevada is primarily dictated by the frequency of spalling during range fires (*13*). The progressive shedding of individual grains or crystals also contributes to boulder attrition. Subsurface weathering rates depend largely on the abundance of moisture available for diverse chemical weathering processes in this relatively dry region. Moisture is retained just below the soil surface for appreciable periods after rainstorms and during snow melt, giving rise to a near-surface zone where weathering is significant and a zone below where weathering is negligible. This notion is consistent with observations of maximum depths of soil development ranging from 1.4 to 1.9 m on these moraines (*11*). Weathering is generally a prelude both to attrition due to spalling and to granular disintegration soon after exposure to the elements.

Rates of boulder weathering and attrition are poorly known. Under modern conditions, spalling erodes exposed granitic boulders at rates estimated up to $2 \times 10^{-6}$ to $4 \times 10^{-6}$ m/year (*13*). On a Mono Basin moraine, a subsurface boulder with a diameter of 0.5 m was thoroughly disintegrated; observed subsurface boulders, which were smaller, were in a similar state on both Mono Basin and Tahoe moraines (*8*). This finding suggests that subsurface weathering rates are substantially faster than $1.3 \times 10^{-6}$ m/year and probably significantly faster than surface rates.

The model simplifies the effects of weathering and attrition of boulders by combining them into an effective size reduction of boulders. It tracks the size of spherical boulders that effectively lose thin surface layers while they reside both in the relatively active subsurface weathering zone and on the ground surface. A boulder disappears from the moraine surface when its radius vanishes. It is convenient to consider boulders of uniform size, herein taken to be 0.5 m in diameter, which are uniformly distributed throughout the moraine. As a first approximation, effective boulder attrition rates are assumed to be constant in time. A rate is assumed for the attrition of exposed boulders and a single higher rate is taken for subsurface boulders within 2 m of the surface, on the assumption that this rate is negligible at greater depth.

In spite of extreme idealizations, model results reproduce the essence of several known properties of boulder abundance and exposure ages (Fig. 2). The disappearance of surface boulders because of the complete wastage predicted by the model is consistent with two widely recognized trends on moraines of increasing age: a decrease in surficial boulder abundance and an increase in the representation of boulders of weathering-resistant lithologies (*7, 23*). Moraines of a given age are associated with a range of exposure ages, as has been observed (*5, 14*). The mean exposure age of boulders on a moraine crest is always only a fraction of the moraine age, although the two ages become identical for very young moraines. On moraines sufficiently old that most boulders originally on the surface have been destroyed by weathering, exposure ages would be substantially younger than the moraine and, hence, would be useful in establishing only minimum moraine ages.

Mean exposure age does not necessarily increase with time because of the complicated interplay between rates at which boulders are unearthed and are reduced in size, both of which generally vary with time (Fig. 2B). Early in the aging of a moraine, exposure ages of boulders range from the actual moraine age represented by boulders originally on the surface to very young ages for freshly unearthed boulders; mean age increases with time. Later, as the moraine form becomes more subdued and stable, rates at which the moraine crest subsides diminish. As a result, boulders emerging at the crest surface are increasingly weathered, having spent more time in the relatively reactive subsurface weathering zone. The longevity of these less coherent surface boulders is reduced, which together with the selective disappearance of older boulders decreases the mean exposure age of surface boulders. The possibility that mean exposure ages of boulders on the crest of a younger moraine could exceed those on an older moraine was apparently not considered by Phillips and co-workers (*5*), who interpreted their cosmogenic dates as suggesting that the previously accepted chronology for the older moraines should be reversed (Fig. 2A).

Factors absent from the model, such as the attritional loss of cosmogenically enriched outer parts of boulders and prior exposure, introduce additional uncertainty into the interpretation of cosmogenic surface exposure ages. In view of these complications and uncertainties, chronologies based on cosmogenically determined boulder ages may generally differ from lateral moraine-age sequences that are based on geomorphic arguments and stratigraphy. Such differences, rather than complete accord, are to be expected, particularly for older moraines. Contrary to common assertions (*14*), moraines with identical exposure ages are not necessarily correlative (Fig. 2B).

Our model yields considerable insight into the diverse consequences of erosion and weathering on exposure-age dating of moraines and provides ample motivation for refining the modeling of these processes. More generally, our theoretical considerations highlight the need to complement advances in the use of cosmogenic isotopes to date geomorphic surfaces with detailed examination of the dynamic nature of landforms and of the universally present processes of weathering, erosion, and deposition.

### REFERENCES AND NOTES


1. D. Lal, *Annu. Rev. Earth Planet. Sci.* **16**, 355 (1988).
2. P. R. Bierman, *J. Geophys. Res.*, in press.
3. K. Nishiizumi *et al.*, *ibid.* **94**, 907 (1989).
4. A. R. Gillespie and P. R. Bierman, unpublished results.
5. F. M. Phillips *et al.*, *Science* **248**, 1529 (1990).
6. E. Blackwelder, *Geol. Soc. Am. Bull.* **42**, 865 (1931).
7. R. P. Sharp and J. H. Birman, *ibid.* **74**, 1079 (1963).
8. R. M. Burke and P. W. Birkeland, *Quat. Res.* **11**, 21 (1979).
9. A. R. Gillespie, thesis, California Institute of Technology (1982); R. Crook and A. R. Gillespie, in *Rates of Chemical Weathering of Rocks and Minerals*, S. M. Colman and D. P. Dethier, Eds. (Academic Press, San Diego, CA, 1986), pp. 395–417.
10. M. I. Bursik and A. R. Gillespie, *Quat. Res.* **39**, 24 (1993).
11. P. W. Birkeland and R. M. Burke, *Arct. Alp. Res.* **20**, 473 (1988).
12. The local mean annual precipitation is 450 mm. Modern vegetation consists of mixed conifer forest with an understory of Great Basin sage community.
13. P. Bierman and A. Gillespie, *Geology* **19**, 641 (1991).
14. M. G. Zreda and F. M. Phillips, *Eos* (fall meeting) **74**, 292 (abstr.) (1993).
15. S. M. Colman and K. L. Pierce, *Quat. Res.* **25**, 25 (1986).
16. T. C. Meierding, in *Correlation of Quaternary Chronologies*, W. C. Mahaney, Ed. (Geo Books, Norwich, UK, 1984), pp. 455–477.
17. R. S. Anderson and N. F. Humphrey, in *Quantitative Dynamic Stratigraphy*, T. A. Cross, Ed. (Prentice-Hall, Englewood Cliffs, NJ, 1989), chap. 19. For a more general introduction to diffusional modeling of topography, see M. A. Carson and M. J. Kirkby, *Hillslope Form and Process* (Cambridge Univ. Press, New York, 1972).
18. Boulders are assumed not to move downslope because erosional processes that probably dominate in transferring material downslope in this climatic region (soil creep, wind scour, rain splash) operate on a scale much smaller than that needed to move boulders. Field observations support this assumption: If boulders were moving downslope they would accumulate at the foot of the moraine, but this is not the case.
19. This relation is applicable for any soil-moving process and for motion restricted down the fall line, which is appropriate because lateral moraines are long ridges adequately modeled by the consideration of only the soil transfer perpendicular to the moraine axis.
20. K. L. Pierce and S. M. Colman, *Geol. Soc. Am. Bull.* **97**, 869 (1986). The κ increase with slope length presumably reflects the increasing importance of slope length–dependent sediment transport by sheet wash and rilling.
21. T. C. Hanks *et al.*, *J. Geophys. Res.* **89**, 5771 (1984).
22. T. Swanson, personal communication.
23. R. P. Sharp, *Geol. Soc. Am. Bull.* **83**, 2233 (1972).


24. We thank A. Gillespie for his interest and encouragement; T. Swanson for his unpublished topographic profiles; and D. Clark, A. Heyneman, T. Swanson, and especially A. Gillespie for thoughtful reviews and suggestions. Supported by the National Science Foundation and Academy of Finland.

22 March 1994; accepted 29 June 1994


# Controlling Molecular Order in "Hairy-Rod" Langmuir-Blodgett Films: A Polarization-Modulation Microscopy Study


V. K. Gupta, J. A. Kornfield,* A. Ferencz, G. Wegner



**The interplay of molecular weight, layer thickness, and thermal annealing in controlling molecular order in ultrathin Langmuir-Blodgett films is characterized with the use of polarization-modulation laser-scanning microscopy. The degree and direction of molecular alignment can be imaged rapidly and sensitively through the magnitude and orientation of linear dichroism in Langmuir-Blodgett films of rodlike poly(phthalocyaninatosiloxane) (PcPS). Images are presented for films as thin as two molecular layers (~44 angstroms). Molecular alignment along the transfer direction is much stronger for films of PcPS with ~25 repeat units (~10 nanometers long) than for those with ~50 repeat units (~20 nanometers long). Enhancement of alignment by thermal annealing is also much greater for PcPS-25 than PcPS-50. Intimate interaction with the substrate suppresses improvement in alignment by annealing, evident by an anomalously small increase in anisotropic absorption of the first two layers.**


Molecular orientation plays a key role in the combined areas of polymer physics, condensed matter physics, and thin-film technology because it determines the useful properties of a large class of materials. For example, a high degree of alignment is the basis of improved mechanical, optical, and electrical properties in almost all polymers and in the technological application of liquid crystalline and other mesoscale-ordered systems. Consequently, it is necessary to understand the correlations among molecular order, material properties, and fabrication procedures. Toward this end, we developed an optical technique to image molecular order and study Langmuir-Blodgett (LB) films of a rigid-rod polymer.

The high degree of order in LB films opens potential applications as nonlinear optical systems, molecular templates for protein crystallization, insulating or patterning layers in microelectronic devices, and selective layers in biosensors (*1*). Experimental characterization of the degree and direction of alignment in films as thin as a few nanometers is required in order to understand how molecular design and processing strategies lead to the ultimate state of alignment.

Various spectroscopic methods have been used to examine the structure, properties, and molecular arrangement of LB films (*1, 2*); however, detailed characterization of molecular order has been lacking because these spectroscopic techniques average over large areas of films a


V. K. Gupta and J. A. Kornfield, Division of Chemistry and Chemical Engineering, California Institute of Technology, Pasadena, CA 91125, USA.
A. Ferencz and G. Wegner, Max-Planck-Institut für Polymerforschung, Postfach 3148, D-6500 Mainz, Germany.

*To whom correspondence should be addressed.